

Interfacial reactions between sapphire and Ag–Cu–Ti-based active braze alloys

Majed Ali^{a,*}, Kevin M. Knowles^a, Phillip M. Mallinson^b, John A. Fernie^{b,c}

^aDepartment of Materials Science and Metallurgy, University of Cambridge,
27 Charles Babbage Road, Cambridge, CB3 0FS, UK

^bMaterials Science, AWE, Aldermaston, Reading, Berkshire, RG7 4PR, UK

^cNow at Lucideon Limited, Queens Road, Penkhull, Stoke-on-Trent, Staffordshire
ST4 7LQ, UK

*Corresponding author: Tel.: +44 (0)1223 334357

E-mail address: ma591@cam.ac.uk

Abstract

The interfacial reactions between two commercially available Ag–Cu–Ti-based active braze alloys and sapphire have been studied. In separate experiments, Ag–35.3Cu–1.8Ti wt.% and Ag–26.7Cu–4.5Ti wt.% alloys have been sandwiched between pieces of R-plane orientated sapphire and heated in argon to temperatures between 750 and 900 °C for 1 min. The phases at the Ag–Cu–Ti/sapphire interfaces have been studied using selected area electron diffraction, energy dispersive X-ray spectroscopy and electron energy loss spectroscopy.

Gradual and subtle changes at the Ag–Cu–Ti/sapphire interfaces were observed as a function of temperature, along with the formation of a transient phase that permitted wetting of the sapphire. Unequivocal evidence is shown that when the active braze alloys melt, titanium first migrates to the sapphire and reacts to dissolve up to ~33 at.% oxygen, forming a nanometre-size polycrystalline layer with a chemical composition of Ti_2O_{1-x} ($x \ll 1$). Ti_3Cu_3O particles subsequently nucleate behind the Ti_2O_{1-x} layer and grow to become a continuous micrometre-size layer, replacing the Ti_2O_{1-x} layer. Finally at 845 °C, a nanometre-size γ -TiO layer forms on the sapphire to leave a typical interfacial structure of Ag–Cu/ Ti_3Cu_3O / γ -TiO/sapphire consistent with that seen in samples of polycrystalline alumina joined to itself with these active braze alloys. These experimental observations have been used to establish a definitive bonding mechanism for the joining of sapphire with Ag–Cu alloys activated by small amounts of titanium.

1. Introduction

Active metal brazing is a versatile technique to join a wide range of ceramics to themselves or to metals. In this technique, an alloy containing a small amount of an element that permits a reaction between it and the ceramic whilst in the molten state is used. Such an element is commonly referred to as an active

element, and the resultant braze alloy is called an active braze alloy (ABA). Wetting of the ceramic and joining of the components is facilitated by the formation of interfacial phases. The ABA may be selected from a wide range of commercially available ABAs, such that the ABA reacts to form uniform and continuous reaction layers. This is ideally achieved without forming excessive amounts of brittle interfacial phases over a relatively short period of time at the bonding temperature. A review of the state of knowledge of some commonly used commercially available brazes and ABAs and their reactivity with various engineering ceramics, can be found in a paper by Fernie et al. [1].

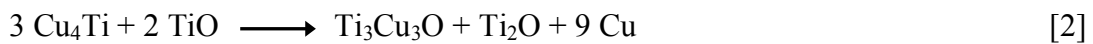
ABAs are typically based on Ag, Cu, Ni or Au and often contain Ti as the active element. The various braze families offer very different temperature capabilities. The most commonly used ABAs are based on Cu and Ag–Cu with additions of Ti, particularly for the joining of alumina. Two widely used Ag–Cu–Ti alloys are Ag–35.25Cu–1.75Ti wt.% and Ag–26.7Cu–4.5Ti wt.%, known by their trade names of Cusil ABA® and Ticusil®, respectively. The addition of small amounts of Ti to eutectic Ag–28Cu wt.%, or near-eutectic Ag–Cu alloys, is one effective method to overcome the issues of wetting the ceramic with the Ag–Cu alloy, as indicated by the widespread use of such alloys with a broad range of ceramics [1–5]. The approach of alloying the Ti with Ag–Cu, or cladding it with Ag–Cu, protects the Ti from oxidising by a reaction between it and any gases in the furnace. Consequently, almost all of the Ti is available for wetting the ceramic, and therefore only small amounts of Ti are needed to form the joint. Both of these approaches are used separately to prepare Cusil ABA® and Ticusil® respectively. The Ti in Cusil ABA® is in the form of Cu₄Ti, with grains of Cu₄Ti randomly distributed amongst the Ag–Cu eutectic alloy. In Ticusil®, the Ti is in the form of a thin foil that is encased by eutectic Ag–Cu [2].

Several groups [2,6,7] have studied the interfacial phases formed between Cusil ABA® and alumina, and Ticusil® and alumina, typically after brazing the alumina to itself rather than to a metal. This approach has been used to eliminate metal dissolution into the ABAs, therefore allowing the natural interaction between the ABAs and the alumina to be studied. A continuous bilayer is typically observed on the alumina, consisting of a nanometre-size titanium oxide layer on the alumina and a micron-size Ti₃Cu₃O layer in contact with the ABA [2,6,7]. A recent investigation by transmission electron microscopy (TEM) of Cusil ABA®/alumina and Ticusil®/alumina interfaces that were heated to temperatures between 815 and 900 °C for 2 to 300 min confirmed that the titanium oxide layer on the alumina is mostly composed of γ -TiO grains [2]. It was apparent that further titanium oxides such as Ti₃O₂ could also be present, but as very minor components of this layer. The Ti₃Cu₃O phase was also shown to be less stable at the peak temperatures used compared with γ -TiO. Another aspect common in the literature is the identification of small amounts of Al in Ti₃Cu₃O [6-8]. This is normally accounted for by the work of Kelkar and Carim [8], which suggests that Cu in Ti₃Cu₃O is substituted by the Al. This is supported

by the observation that the Ti and Cu+Al contents are usually approximately equal.

The extent to which silica and calcium silicate secondary phases in the alumina, up to a level of about 5 wt.%, participate in the reactions at the braze/alumina has been determined in a previous study [2]. Si and Ca from the secondary phases have been shown to form solid solutions with Ti_3Cu_3O and γ -TiO, respectively. Consequently, the interfacial structure is not significantly affected by reducing the purity of the alumina by such a relatively small amount.

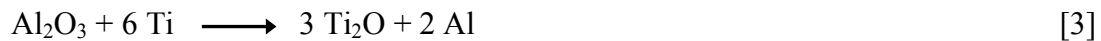
Although there is extensive scientific literature available on the Ag-Cu-Ti/alumina system [2,6–19], the evolution of the interfacial phases is still not fully understood. This is apparent from the clear discrepancies in the reaction mechanisms provided in the literature, which are reviewed here. Lin et al. [7] provided two mechanisms from an investigation of the interfacial phases formed between 99.99 wt.% Al_2O_3 and Cusil ABA® and Ticusil®, after heating to temperatures that were 15 °C above the liquidus temperatures of the ABAs. The first mechanism proposed by Lin et al. [7] was initially proposed by Suenaga et al. [20] for reactions that occur between a series of Ag-Cu/Ti bilayer thin films which were deposited on sapphire. In this mechanism, Ti reacts with the alumina to form TiO, liberating some Al to an unspecified location. During the bonding process, Ti also reacts with Cu to form Cu_4Ti , which subsequently goes on to react with the TiO to form Ti_3Cu_3O and Ti_2O on cooling the joints. This first mechanism is described by equations 1 and 2.



However, on the basis of oxidation-reduction reactions alone, the Ti should not react with the ceramic. The change in free energy for equation 1 at a temperature of 830 °C, which was used to join alumina with Cusil ABA®, is positive and approximately 5.5 kJ mol⁻¹.

The second mechanism proposed by Lin et al. [7] begins in a similar manner, but Ti_2O is formed rather than TiO. However, the titanium oxide observed in joints by Lin et al. [7] was misidentified as Ti_2O , rather than Ti_3O_2 . All of the electron diffraction patterns provided by Lin et al [7] which were used to identify the crystal structure of the titanium oxide are consistent with the crystal structure of Ti_3O_2 (hexagonal, $P6/mmm$, space group 191, $a = 4.99 \text{ \AA}$ and $c = 2.88 \text{ \AA}$) rather than the crystal structure of Ti_2O (trigonal, $P\bar{3}m1$, space group 164, as indexed on the basis of a hexagonal unit cell $a = 2.96 \text{ \AA}$ and $c = 4.85 \text{ \AA}$) or that of α -Ti (hexagonal, $P6_3/mmc$, space group 194, $a = 2.96 \text{ \AA}$ and $c = 4.85 \text{ \AA}$) if the oxygen was considered to be a solute in α -Ti. It was suggested that Ti_2O on the

alumina subsequently reacts with Cu on cooling to form $\text{Ti}_3\text{Cu}_3\text{O}$. This mechanism is represented by the two reactions:



where the location of the oxygen liberated in equation 4 is not specified. The Ti_2O formed by equation 3 is Ti with added O in solid solution. The formation of such a solid solution could make this reaction energetically possible. A mechanism of this kind would be consistent with the observation that the titanium oxide layer on the alumina is much thinner than the $\text{Ti}_3\text{Cu}_3\text{O}$ layer. It is worth noting that clear changes in the thickness and the structure of the $\text{Ti}_3\text{Cu}_3\text{O}$ layer have been observed by altering the length of time alumina/Cusil ABA®/alumina joints are held at the peak temperature of a brazing cycle [2]. These changes in the $\text{Ti}_3\text{Cu}_3\text{O}$ layer indicate that the layer is formed at the peak temperature and not during the cooling process.

Stephens et al. [6] take the formation free energy of $\text{Ti}_3\text{Cu}_3\text{O}$ into account to explain the reaction of Ti with alumina by equation 1. It was suggested that the sum of the change in free energy for equation 1 and the formation free energy of $\text{Ti}_3\text{Cu}_3\text{O}$, which was assumed to form at the bonding temperature by equation 5 below, produces an overall negative value.



The driving force was then a reduction in free energy of the system as a result of all the interfacial reactions if the titanium oxide and $\text{Ti}_3\text{Cu}_3\text{O}$ formed at the same time. However, it has been shown that a Ag–Cu–Ti alloy with a low Ti content (0.7 at.%) can react with sapphire at 900 °C in a sessile drop configuration to form a titanium oxide layer by itself on the sapphire [21]. Therefore, this mechanism does not agree with all of the experimental observations.

All of these reaction mechanisms have been proposed on the basis of characterising single ABA/ Al_2O_3 interfaces, each of which has been prepared using disparate brazing conditions. Thus, only 'snapshots' of the state of the interfacial phases have been reported and in each case a continuous interfacial bilayer, as described above, was observed. This is because the interfacial phases evolve very quickly at the bonding temperature, in particular the $\text{Ti}_3\text{Cu}_3\text{O}$ layer, and are well developed within 2 min at the liquidus temperature of the ABA [2].

This work aims to clarify the reaction processes occurring between Al_2O_3 and Cusil ABA® and Ticusil® leading to the interfacial microstructures seen in Al_2O_3 /ABA/ Al_2O_3 joints. The approach used to study the evolution of the

interfacial phases has combined the use of a short brazing time of 1 min with relatively fast heating and cooling rates to join sapphire to itself with each ABA. Single crystals of Al₂O₃, in the R-plane orientation, rather than polycrystalline Al₂O₃ were joined together by the ABAs to eliminate chemical reactions that might occur between the ABAs and any secondary phases in the polycrystalline material. Since no definitive relationships between the orientation of the sapphire and the particles nucleating on it were identifiable, other orientations of sapphire were not examined. The components were heated to temperatures between 750 and 900 °C. This range was used to study the state of the ABA/sapphire interfaces after heating to temperatures slightly below the solidus temperatures of the ABAs through to temperatures equal to or exceeding their liquidus temperatures. Therefore, it was expected that this approach would result in gradual changes at the ABA/sapphire interfaces.

2. Experimental

2.1. Materials

R-plane (1 $\bar{1}$ 02) oriented sapphire was joined to itself using two commercially available Ag–Cu–Ti-based ABAs. The sapphire substrates were supplied by the MTI Corporation (USA) at a purity of >99.99 wt.% and in the form of a 0.5 mm thick wafer with a diameter of about 50 mm. The average surface roughness was measured using a profilometer (Dektak 6 M stylus profiler, Veeco, USA) at 250 nm. The wafer was carefully cut to produce 10 × 5 × 0.5 mm substrates for joining.

The ABAs, Cusil ABA® (Ag–35.3Cu–1.8Ti wt.%) and Ticusil® (Ag–26.7Cu–4.5Ti wt.%), were supplied by VBC Group Ltd (UK) in foil form, with a thickness of ~50 µm, from which 10 × 5 mm sections were taken for joining. Cusil ABA® contained Cu₄Ti grains randomly distributed amongst eutectic Ag–Cu. Ticusil® had a Ag–Cu eutectic/Ti/Ag–Cu eutectic structure where the thickness of the Ti layer varied between ~50 nm to 10 µm. Prior to brazing, the sapphire substrates and ABAs were cleaned in detergent and placed in an ultrasonic bath for up to ~15 min.

2.2. Brazing procedure

Brazing was performed in an atmosphere of purified argon, which was established in a horizontal electric furnace (STF 15/450, Carbolite, UK). Argon gas was purified using the BIP® technology by Air Products and Chemicals (USA), after which it was then introduced to the furnace. This purification process reduces the concentrations of O₂ and H₂O to less than 10 and 20 ppb, respectively. A purging procedure was used to prepare the furnace for the brazing experiments. This initially involved evacuating the furnace to a rough vacuum before cleaning with purified argon, which was repeated three times,

and then allowing the gas to flow through the furnace for ~20 min before starting a brazing cycle. A heating rate of 35 °C min⁻¹ was used. The cooling rate was ~30 °C min⁻¹ between the peak temperature used and ~500 °C, after which it reduced significantly during a furnace cool to room temperature.

In all cases, a sapphire/ABA/sapphire configuration was used with a pressure of ~4 kPa applied to the joints using a 20 g weight. Joints made with Cusil ABA[®] were heated to 750, 800, 815 and 845 °C, while those made with Ticusil[®] were heated to 750, 800, 815, 845 and 900 °C. The components were all held at the peak temperature for 1 min.

2.3 Analytical procedures

Cross-sections of the ABAs and the joints were examined using scanning electron microscopy (SEM) and energy dispersive X-ray spectroscopy (EDS) before more detailed examinations were undertaken by TEM. Samples for SEM analysis were mounted in an acrylic polymer at room temperature, polished using standard metallographic techniques and then coated with a thin layer of carbon. Three, or more, cross-sections from each sample were analysed using a field emission scanning electron microscope (Leo 1530 VP, Leo Electron Microscopy - Carl Zeiss, Germany) operated at 20 keV. This microscope was equipped with an energy dispersive spectrometer (INCA-7426, Oxford Instruments, UK), which was particularly useful to identify residual Cu₄Ti grains in the Cu-rich phase of Cusil ABA[®]. This is because these phases have a similar average atomic number, and therefore they look very similar in a backscattered electron image (BSEI).

Thin sections of ABA/sapphire interface for TEM analysis were prepared using a focussed ion beam (FIB) instrument (Helios Nanolab, FEI, USA). A procedure that is commonly referred to as the lift-out technique [22] was used to transfer 10 × 5 µm sections of ABA/sapphire interface to Mo grids, or a carbon substrate on a Mo grid. These sections were reduced to a thickness between 30 and 100 nm by the FIB. Elemental analysis of the thin sections was performed in a FEI Tecnai Osiris FEG STEM (USA), which was operated at 200 keV. This microscope was fitted with an EDS system with four windowless Bruker silicon drift detectors (Super-X system, FEI, USA), which permitted the detection of weak and low energy X-rays such as O K_α. In addition to bright field imaging, atomic number contrast imaging was performed using a high angle annular dark field (HAADF) detector.

Electron energy loss spectroscopy (EELS) was used to estimate the relative amounts of Ti and O in an interfacial phase that formed in an early stage of the bonding process. Electron energy loss (EEL) spectra were collected with a Gatan Enfinium ER 977 spectrometer attached to the FEI Tecnai Osiris FEG STEM. The energy resolution of the Schottky field-emitter, defined as the full width at half-maximum height of the zero-loss peak, was between 1.3 and 1.5 eV. The relative sample thickness t/λ , as estimated from the low-loss spectra, was between 0.4

and 0.7. Measurements were collected in diffraction mode far away from zone axes to ensure that they were not dependent on the orientation of the sample. An illumination semi-angle α of 7.2 mrad, a collection semi-angle β of 3.8 mrad and an entrance aperture of 2.5 mm were used. An inverse power law background was subtracted and plural scattering contributions were removed using the Fourier-ratio deconvolution technique.

A JEOL 200CX (Japan) transmission electron microscope was used to acquire selected area diffraction patterns from the interfacial phases. The smallest area of analysis was equivalent to that of a circle with a diameter of 500 nm. This area was typically significantly larger than the grains studied. Therefore most of the diffraction patterns presented in this work have been presented alongside a schematic to clearly show the relevant reflections. An Al thin film, supplied by Agar Scientific (UK), was used to monitor the camera length of the microscope at regular intervals.

3. Results

The appearance of the ABAs as-received and after heating to temperatures between 750 and 900 °C for 1 min can be seen in Figure 1. Before heating, the surfaces of Cusil ABA® and Ticusil® had a faint copper-coloured appearance. After heating to 750 °C, the surfaces of the ABAs did not change in appearance. Cross-sections of the ABAs before and after heating to 750 °C are shown in the BSEIs given in Figure 2. As expected, there is evidence of solid-state diffusion in the ABAs at this temperature. In both ABAs, the lamellar eutectic structure of Ag and Cu was transformed to leave agglomerates of Cu within a Ag matrix. The random distribution of Cu₄Ti in Cusil ABA® was unaffected. Initially, Ticusil® had isolated particles of Cu₄Ti₃ along the Ti/Ag–Cu interfaces. On heating, a reaction at these interfaces between Cu and Ti resulted in the formation of a continuous Cu₄Ti₃ layer alongside the Ti layer that extended through the ABA. At 750 °C, the titanium in the ABAs could not diffuse to the ABA/sapphire interfaces. Consequently no interfacial phases were observed and ultimately no bond was formed between the ABAs and the sapphire.

Joining occurred on melting of the ABAs, which was accompanied by a distinctive change in their appearance. On heating to 800 °C, the ABAs had partially melted because the temperature was between the solidus temperature of the alloys (i.e. 780 °C) and their liquidus temperatures (i.e. 815 °C for Cusil ABA® and 900 °C for Ticusil®). At areas where melting had occurred, the ABA/sapphire interface, viewed through one of the sapphire pieces, was dark grey. The appearance from this view was consistently dark grey regardless of the peak temperature used (Figure 1). A collection of BSEIs of sapphire/Cusil ABA®/sapphire joints prepared with a peak temperature between 800 and 845 °C are shown in Figure 3. It is evident from the BSEIs in Figure 3a that Cusil

ABA® had only partially melted at 800 °C because small grains of Cu₄Ti were observed in the ABA.

Using a peak temperature of 800 °C resulted in the formation of a polycrystalline layer, about 130 nm thick, on the sapphire. A HAADF image of this layer is shown in Figure 4, alongside the corresponding EDS maps for the elements present. EDS analysis indicated that Ti and O were components of this layer, with a typical composition of 69Ti–29O–2Cu at.%. A selection of electron diffraction patterns acquired from this layer is shown in Figure 5; the patterns have been indexed on the basis of a hexagonal cell with $a = 2.96 \text{ \AA}$ and $c = 4.85 \text{ \AA}$. These patterns are consistent with two different crystal structures, each being based on a solution of O in Ti. One of these structures is that of α -Ti (hexagonal, $P6_3/mmc$, space group 194) with a random distribution of O atoms in the octahedral interstices of the metal lattice. The other structure is formed on ordering of the O atoms to occupy every second layer of octahedral interstices extending normally to the c -axis of the metal lattice, as described by Holmberg [23]. This displaces the Ti atoms that are adjacent to the O atoms in a direction parallel to the c -axis, and therefore away from their ideal positions in the hexagonal closed-packed arrangement. The result is a structure that can be described by a rhombohedral unit cell of Ti₂O (trigonal, $P\bar{3}m1$, space group 164). It is possible for reflections that are forbidden by the space group symmetry of α -Ti, such as $11\bar{2}\bar{1}$ and $2\bar{1}\bar{1}1$ in the $[\bar{1}2\bar{1}3]$ pattern, to occur by double diffraction. Since small amounts of Al were found in the ABA within a region of $\sim 1.5 \text{ \mu m}$ from the ABA/sapphire interface it can be established that Ti dissolves O from the sapphire rather than from low levels of oxygen impurity in the Ar atmosphere in the furnace. Aluminium was found at a level of $\sim 2 \text{ at.}\%$ in the Ag-rich phase of the ABA and at $\sim 0.5 \text{ at.}\%$ in the Cu-rich phase. In this work, it is not clear whether the O in Ti has an ordered or random arrangement. The phase analysis performed by X-ray methods on the Ti-O system up to $\sim 33 \text{ at.}\%$ O by Holmberg [23] and Andersson et al. [24] revealed the existence of ordered solutions at such high proportions of O. Their results suggest that ordering of O is likely in the Ti-rich layer found on the sapphire.

EELS was used to estimate the Ti and O content in the reaction layer and to confirm that it was a solid solution of O in Ti. The Ti L and O K edges were compared to their energy values recorded with $\sim 99.5 \text{ wt.}\%$ α -Ti that contained $\sim 0.4 \text{ wt.}\%$ O as a solute; the remainder being N, H, Fe and C. Lainé and Knowles [25] provided the α -Ti reference material and they report its full chemical composition from a combination of combustion analysis and inductively coupled plasma optical emission spectroscopy in their work. A thin foil of α -Ti was prepared for EELS analysis using the same procedure used for preparing thin foils of ABA/sapphire interface. In addition, the α -Ti reference was positioned on the same grid that held the ABA/sapphire interface that was heated to 800 °C, in order to use the same electron beam conditions for the analysis of the reaction layer and the reference material. EEL spectra showing the Ti L and O K edges for

the reaction layer and α -Ti are given in Figure 6 and the energy positions of these edges are given in Table 1. Stoyanov et al. [26] have compared Ti L and O K EEL near-edge structure of seven different titanium oxides with valence states for Ti ranging between +2 and +4. It was found that the onset of the Ti L edge shifts to lower energy with decreasing oxidation state by about 1.7–2.0 eV per oxidation state. No decrease in energy of the Ti L edge was observed in this work. The energy positions of the Ti L and O K edges for the reaction layer and α -Ti reference material are almost identical. Therefore, it is concluded that this layer is a solid solution of a significant quantity of O in Ti. The Ti/O ratio for this layer varied between 2.5 and 2.1. The O atoms are probably ordered in Ti at such high concentrations of O, as described above for Ti_2O . Since the concentration of O is only slightly lower than the limiting solubility of O in α -Ti at 800 °C, which is ~ 33 at.% O [27] and is independent of temperature, there would be O vacancies. Therefore, the reaction layer on the sapphire is designated $\text{Ti}_2\text{O}_{1-x}$.

In the same sample, isolated particles of $\text{Ti}_3\text{Cu}_3\text{O}$, about 100 nm in diameter, nucleated on the $\text{Ti}_2\text{O}_{1-x}$ layer and were in contact with the ABA as shown in Figure 4. The crystal structure of these particles was identified as that of $\text{Ti}_3\text{Cu}_3\text{O}$ (cubic, $Fd\bar{3}m$, space group 227) with a unit cell length of 11.2–11.3 Å. A selection of electron diffraction patterns from this phase is shown in Figure 7. A typical composition was 45.3Ti–41.2Cu–1.4Al–12.1O at.%, which is consistent with $\text{Ti}_3\text{Cu}_3\text{O}$ containing a small amount of aluminium as a solute.

An increase in the peak temperature to 815 °C caused growth of $\text{Ti}_3\text{Cu}_3\text{O}$ that was dominated by lateral growth to form a 700 nm thick continuous layer. At the same time, the $\text{Ti}_2\text{O}_{1-x}$ layer broke down into separate particles. Small $\text{Ti}_2\text{O}_{1-x}$ particles, about 5–30 nm in diameter (assuming equiaxed grains), were on the sapphire and larger particles, about 50–100 nm in diameter, were in contact with the $\text{Ti}_3\text{Cu}_3\text{O}$ layer. Occasionally, $\text{Ti}_2\text{O}_{1-x}$ particles up to 500 nm wide were found within the $\text{Ti}_3\text{Cu}_3\text{O}$ layer. Increasing the peak temperature to 845 °C produced an 860 nm thick $\text{Ti}_3\text{Cu}_3\text{O}$ layer in contact with the ABA and a 50 nm thick γ -TiO layer on the sapphire. A selection of electron diffraction patterns from γ -TiO (cubic, $Fm\bar{3}m$, space group 225, $a = 4.2$ Å) is shown in Figure 8. Isolated $\text{Ti}_2\text{O}_{1-x}$ particles were occasionally observed between the $\text{Ti}_3\text{Cu}_3\text{O}$ and γ -TiO layers to leave a microstructure very similar to that observed by Stephens et al. [6], when Cusil ABA® was held at 845 °C for 6 min on sapphire. Stephens et al. [6] identified the isolated particles as Ti_2O and they were thought to have formed on cooling by a reaction between titanium in the ABA and γ -TiO.

The composition of $\text{Ti}_3\text{Cu}_3\text{O}$, and the Ag-rich and Cu-rich phases in the ABA near the ABA/sapphire interface did not change beyond a level that could not be accounted for by experimental error when the bonding temperature was increased from 800 to 815 °C. Within a distance of ~ 1.5 μm from the ABA/sapphire interface, the Ag-rich phases contained ~ 15 at.% Cu and ~ 2 at.% Al, while the Cu-rich phases contained less Al, ~ 0.5 at.%, and similar amounts of Ag and Ti. The level of Al in $\text{Ti}_3\text{Cu}_3\text{O}$ increased from ~ 1.5 at.% to 4 at.% with an

increase in the bonding temperature to 845 °C. At the same time, similar amounts of Al were also found in the Ag-rich phase of the ABA within a region of ~2 µm from the ABA/sapphire interface. The Ag-rich phase contained ~15 at.% Cu and ~4 at.% Al. The composition of the Cu-rich phase did not change significantly with this change in temperature.

Similar microstructural developments were observed between Ticusil® and sapphire. A collection of BSEIs of sapphire/Ticusil®/sapphire joints prepared with a peak temperature between 800 and 900 °C are shown in Figure 9. The interfacial structures formed after heating to 800 and 815 °C were very similar. At these temperatures, a continuous Ti₂O_{1-x} layer which was about 150 nm thick formed on the sapphire. Isolated Ti₃Cu₃O particles, up to 100 nm in diameter, were also found between this layer and the ABA. The majority of the Ti in Ticusil® had not reached the interfaces, but remained in the ABA in the form of Cu₄Ti₃ (and also Ti at the peak temperature of 800 °C). At a peak temperature of 845 °C, a continuous 1 µm thick Ti₃Cu₃O layer formed alongside a continuous 30 nm thick γ-TiO layer found on the sapphire. At a peak temperature of 900 °C, there was evidence of small amounts of Cu₄Ti₃ in the ABA as shown in Figure 9d. The Ti₃Cu₃O layer had grown thicker, up to ~1.6 µm, and the γ-TiO layer was ~100 nm at its widest.

4. Discussion

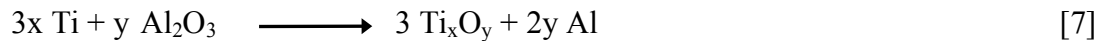
It has been shown that Cusil ABA® and Ticusil® in their molten state react with sapphire by Ti migrating to the surface of the sapphire and dissolving significant amounts of O. The Ti can dissolve O atoms up to a concentration that is essentially equivalent to the formula Ti₂O. This process can be described by equation 3, where the Al that is liberated is dissolved in the ABA, particularly in the Ag-rich phase at a region close to the ABA/sapphire interface. No thermodynamic information on Ti₂O could be found to assess the thermodynamic feasibility of this reaction. It is anticipated that the formation of a solution of O in Ti, and to a lesser degree a solution of Al in Ag, are sufficient, thermodynamically, to drive this reaction. This idea is shared by Moorhead et al. [28], who suggest that the formation of a solution of O in Ti is sufficient by itself to cause dissolution of Al₂O₃ at 1000 °C.

Ti₂O would form as a discontinuous layer by nucleation on the sapphire at random positions. Subsequent growth of the layer would then be dominated by lateral growth until it becomes continuous along the sapphire. At this stage, Ti₃Cu₃O would nucleate on the Ti₂O layer by the reaction:



clearly indicating that Ti_2O is a transient phase during the evolution of the interfacial structure. Again, although there is an estimation of the free energy of formation of Ti_3Cu_3O in the work of Kelkar et al. [29], no experimentally validated thermodynamic information on Ti_3Cu_3O could be found in the literature.

In a recent re-examination of the $Al_2O_3/Ag-Cu-Ti/Al_2O_3$ system [2] it was suggested that the formation of $\gamma-TiO$ on Al_2O_3 occurs by diffusion of Ti through the Ti_3Cu_3O layer by the schematic reaction:



where the Al can form a solid solution with the titanium oxide or Ti_3Cu_3O . This was deduced on the basis that a thinner $\gamma-TiO$ layer formed as the thickness of the Ti_3Cu_3O layer increased. The results in this work also support this idea. Joining sapphire with Cusil ABA® at the peak temperature of 845 °C formed an 860 nm thick Ti_3Cu_3O layer that was in contact with a 50 nm thick $\gamma-TiO$ layer. At the same bonding temperature, using Ticusil® as the ABA resulted in the formation of a thicker Ti_3Cu_3O layer, which was about 1 μm thick, and a slightly thinner $\gamma-TiO$ layer, with a thickness of 30 nm. If $\gamma-TiO$ forms from chemical decomposition/reaction of Ti_2O_{1-x} it would be logical that a thicker $\gamma-TiO$ layer would form in the joint made with Ticusil®. This is because a thicker Ti_2O_{1-x} layer would form initially. However, no experimental evidence has been found to suggest $\gamma-TiO$ forms from Ti_2O_{1-x} . A schematic mechanism for the evolution of the interfacial phases between Cusil ABA® and Ticusil® is shown in Figure 10. An intermediate stage between the disappearance of the Ti_2O_{1-x} phase and the nucleation of $\gamma-TiO$ on the alumina has been given in Figure 10e to suggest that these events are unrelated. It should be noted that this intermediate stage, which shows the presence of Ti_3Cu_3O by itself on the alumina, has not been observed experimentally, and it may be that the $\gamma-TiO$ particles nucleate while some Ti_2O_{1-x} phase is still present. The effect of holding the peak temperature for extended periods of time on the interfacial structure is also summarised in Figure 10 by taking in to account the observations made in an earlier study [2].

5. Conclusions

R-plane orientated sapphire has been brazed to itself using the ABAs Ag-35.3Cu-1.8Ti wt.% and Ag-26.7Cu-4.5Ti wt.% at temperatures between 750 and 900 °C for 1 min. By using a short joining time at temperatures starting slightly below the solidus temperature of the ABAs, along with relatively fast heating and cooling rates, it was possible to study the evolution of the phases at the ABA/sapphire interface. The temperature was increased carefully to result in gradual changes at the interface.

The key result from this work is that on melting of the ABAs, the Ti first reacts with the sapphire to dissolve a significant quantity of O, producing a nanometre-size polycrystalline layer with a chemical composition of Ti_2O_{1-x} ($x \ll 1$). At the same time, the Al released by this initial reaction is dissolved in the ABA, in particular in the Ag-rich phase at regions close to the ABA/sapphire interface. The Ti_2O_{1-x} layer quickly breaks down to permit the growth of Ti_3Cu_3O particles that nucleate on this layer and in contact with the ABA. As a consequence of using relatively long joining times (which means in practice times longer than about 2 min) compared with that used in this work, the Ti_2O_{1-x} phase has not previously been observed as a continuous layer, but instead as isolated particles between layers of Ti_3Cu_3O and γ -TiO. Therefore, Ti_2O_{1-x} has not been previously considered to be a significant phase in the development of the Ti_3Cu_3O/γ -TiO bilayer typically observed on the Al_2O_3 .

Using a peak temperature of 845 °C or higher produced a nanometre-size γ -TiO layer on the sapphire along with a micron-size Ti_3Cu_3O layer in contact with the ABA, consistent with the typical interfacial structure seen in samples of polycrystalline alumina joined to itself. A new reaction mechanism has been provided based on the experimental observations, which describes the formation of a series of metastable phases at the liquidus temperature of the ABAs, such as Ti_2O_{1-x} and Ti_3Cu_3O , and their disappearance so that γ -TiO is left as the most significant interfacial phase for overlong joining times, such as 10 hr at the liquidus temperature of the ABAs.

Acknowledgements

We are grateful for the financial support for this study provided by AWE.

References

- [1] J.A. Fernie, R.A.L. Drew, K.M. Knowles, Joining of engineering ceramics, *Int. Mater. Rev.* 54 (2009) 283–331.
- [2] M. Ali, K.M. Knowles, P.M. Mallinson, J.A. Fernie, Microstructural evolution and characterisation of interfacial phases in $Al_2O_3/Ag-Cu-Ti/Al_2O_3$ braze joints, *Acta Mater.* 96 (2015) 143–158.
- [3] W. Kobsiriphat, S. Barnett, Ag-Cu-Ti braze materials for sealing SOFCs, *J. Fuel Cell Sci. Technol.* 5 (2008) 011002.
- [4] A. Abed, I.S. Jalham, A. Hendry, Wetting and reaction between β' -sialon, stainless steel and Cu–Ag brazing alloys containing Ti, *J. Eur. Ceram. Soc.* 21 (2001) 283–290.

- [5] J. López-Cuevas, J.C. Rendón-Angeles, J.L. Rodríguez-Galicia, M. Herrera-Trejo, J. Méndez-Nonell, High temperature chemical interaction between SSiC substrates and Ag-Cu based liquid alloys in vacuo, *Mater. Sci. Forum* 509 (2006) 111–116.
- [6] J.J. Stephens, F.M. Hosking, T.J. Headley, P.F. Hlava, F.G. Host, Reaction layers and mechanisms for a Ti-activated braze on sapphire, *Metall. Mater. Trans. A* 34 (2003) 2963–2972.
- [7] K-L. Lin, M. Singh, R. Asthana, Interfacial characterization of alumina-to-alumina joints fabricated using silver-copper-titanium interlayers, *Mater. Charact.* 90 (2014), 40–51.
- [8] G.P. Kelkar, A.H. Carim, Al solubility in M_6X compounds in the Ti-Cu-O system, *Mater Lett.* 23 (1995) 231–235.
- [9] S. Hahn, M. Kim, S. Kang, A study of the reliability of brazed Al_2O_3 joint systems, *IEEE Trans. Compon. Packag. Manuf. Technol. Part C* 21 (1998), 211–216.
- [10] W. Byun, H. Kim, Variations of phases and microstructure of reaction products in the interface of $Al_2O_3/Ag-Cu-Ti$ joint system with heat-treatment, *Scr. Metall. Mater.* 31 (1994) 1543–1547.
- [11] D. Janickovic, P. Sebo, P. Duhaj, P. Svec, The rapidly quenched Ag-Cu-Ti ribbons for active joining of ceramics, *Mater. Sci. Eng. A* 304-306 (2001) 569–573.
- [12] A.H. Carim, Convergent-beam electron diffraction “fingerprinting” of M_6X phases at brazed ceramic joints, *Scr. Metall. Mater.* 25 (1991) 51–54.
- [13] M.L. Santella, J.A. Horton, J.J. Pak, Microstructure of alumina brazed with a silver-copper-titanium alloy, *J. Am. Ceram. Soc.* 73 (1990) 1785–1787.
- [14] A. Kar, S. Mandal, R.N. Ghosh, T.K. Ghosh, A.K. Ray, Role of Ti diffusion on the formation of phases in the $Al_2O_3-Al_2O_3$ brazed interface, *J. Mater. Sci.* 42 (2007) 5556–5561.
- [15] S. Mandal, A.K. Ray, A.K. Ray, Correlation between the mechanical properties and the microstructural behaviour of $Al_2O_3-(Ag-Cu-Ti)$ brazed joints, *Mater. Sci. Eng. A* 383 (2004), 235–244.

- [16] W.C. Lee, O.Y. Kwon, C.S. Kang, Microstructural characterization of interfacial reaction products between alumina and braze alloy, *J. Mater. Sci.* 30 (1995), 1679–1688.
- [17] R. Voytovych, F. Robaut, N. Eustathopoulos, The relation between wetting and interfacial chemistry in the CuAgTi/alumina system, *Acta Mater.* 54 (2006) 2205–2214.
- [18] T. Ichimori, C. Iwamoto, S. Tanaka, Nanoscopic analysis of a Ag-Cu-Ti/sapphire brazed interface, *Mater. Sci. Forum* 294-296 (1999) 337–340.
- [19] H. Hongqi, W. Yonglan, J. Zhihao, W. Xiaotian, Interfacial reaction of alumina with Ag-Cu-Ti alloy, *J. Mater. Sci.* 30 (1995) 1233–1239.
- [20] S. Suenaga, M. Nakahashi, M. Maruyama, T. Fukasawa, Interfacial reactions between sapphire and silver-copper-titanium thin film filler metal, *J. Am. Ceram. Soc.* 80 (1997) 439–444.
- [21] R. Voytovych, F. Robaut, N. Eustathopoulos, The relation between wetting and interfacial chemistry in the CuAgTi/alumina system, *Acta Mater.* 54 (2006) 2205–2214.
- [22] L.A. Giannuzzi, F.A. Stevie, A review of focussed ion beam milling techniques for TEM specimen preparation, *Micron* 30 (1999) 197–204.
- [23] B. Holmberg, Disorder and order in solid solutions of oxygen in α -titanium, *Acta Chem. Scand.* 16 (1962) 1245–1250.
- [24] S. Andersson, B. Collén, U. Kuylenstierna, A. Magnéli, Phase analysis studies on the titanium-oxygen system, *Acta Chem. Scand.* 11 (1957) 1641–1652.
- [25] S.J. Lainé, K.M. Knowles, $\{11\bar{2}4\}$ deformation twinning in commercial purity titanium at room temperature, *Philos. Mag.* 95 (2015) 2153–2166.
- [26] E. Stoyanov, F. Langenhorst, G. Steinle-Neumann, The effect of valence state and site geometry on Ti $L_{3,2}$ and O K electron energy-loss spectra of Ti_xO_y phases, *Am. Mineral.* 92 (2007) 577–586.
- [27] H. Okamoto, O-Ti (oxygen-titanium), *J. Phase Equilib. Diff.* 32 (2011) 473–474.
- [28] A.J. Moorhead, H.M. Henson, T.J. Henson, The role of interfacial reactions on the mechanical properties of ceramic brazements, in: J.A. Pask, A.G. Evans (Eds.),

Ceramic microstructures '86: role of interfaces, Springer US, New York, 1987, pp. 949–959.

[29] G.P. Kelkar, K.E. Spear, A.H. Carim, Thermodynamic evaluation of reaction products and layering in brazed alumina joints, J. Mater. Res. 9 (1994) 2244–2250.

	Titanium		Oxygen
	L ₃ edge (eV)	L ₂ edge (eV)	K edge (eV)
Reaction layer	456.5	460.5	531.8
α-Ti	456.0	460.5	532.0

Table 1. Energy positions of the Ti L and O K edges in the reaction layer shown in Figure 4 designated Ti₂O_{1-x} and 99.5 wt.% α-Ti which contains oxygen as an impurity.

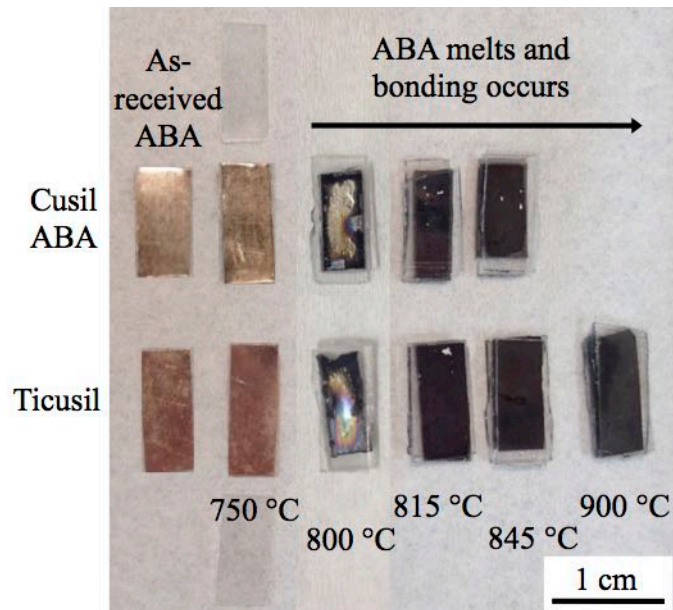


Figure 1. Surfaces of Cusil ABA[®] and Ticusil[®] after holding at temperatures between 750 and 900 °C for 1 min in a sapphire/ABA/sapphire configuration.

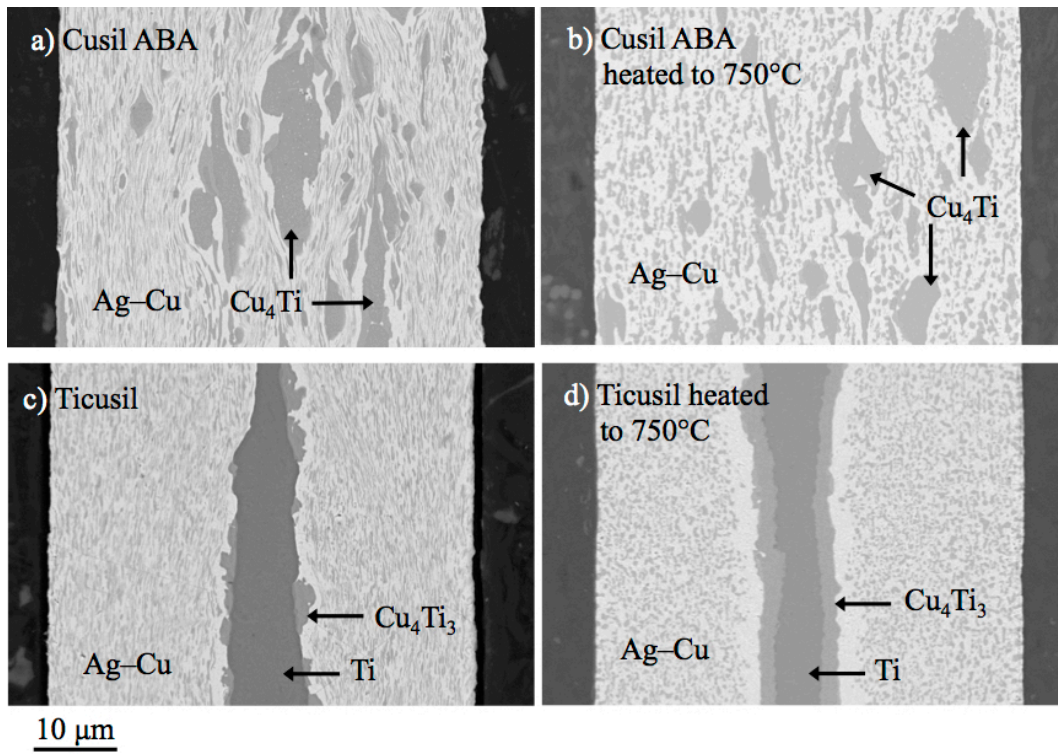


Figure 2. BSEIs of cross-sections of a) Cusil ABA® and c) Ticusil®, and b, d) different cross-sections of the same ABAs after heating to 750 °C for 1 min. In all cases the ABAs are surrounded by acrylic polymer mounting material.

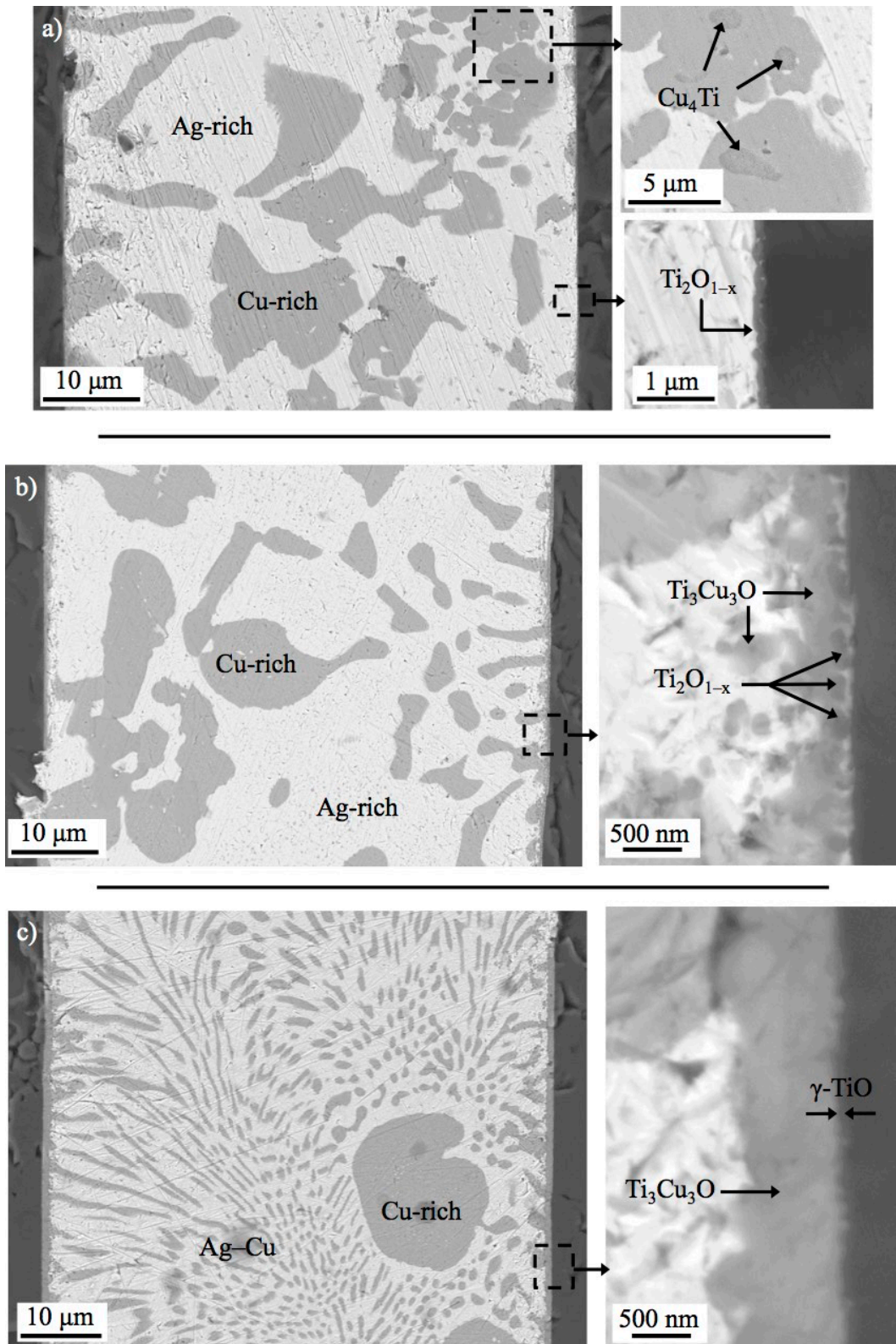


Figure 3. BSEIs of sapphire/Cusil ABA®/sapphire cross-sections which were held at a) 800 °C, b) 815 °C and c) 845 °C for 1 min. Sapphire regions either side of the ABAs appear as either dark grey or black in these BSEIs and also in Figures 4 and

9.

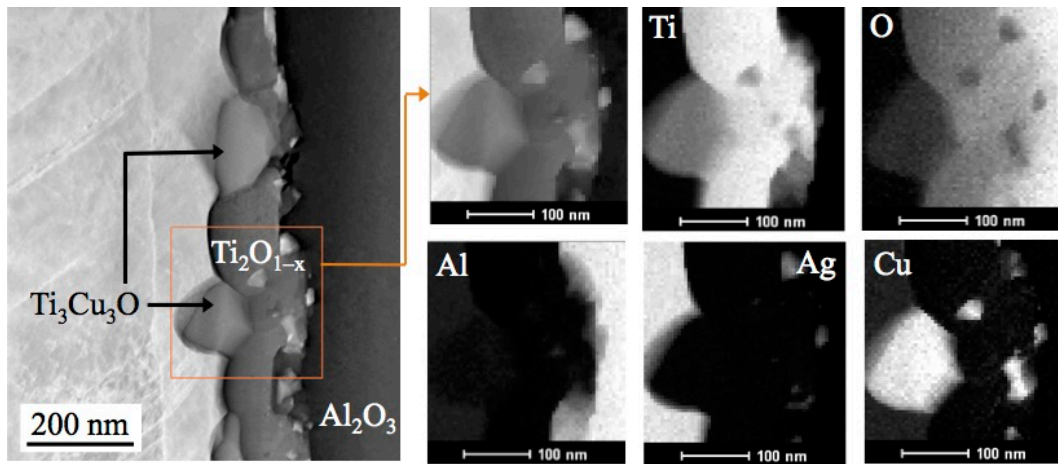


Figure 4. Isolated $\text{Ti}_3\text{Cu}_3\text{O}$ particles on a $\text{Ti}_2\text{O}_{1-x}$ layer formed at a Cusil ABA[®]/sapphire interface after holding at 800 °C for 1 min. The distributions of Ti, O, Al, Ag and Cu are given by their EDS maps.

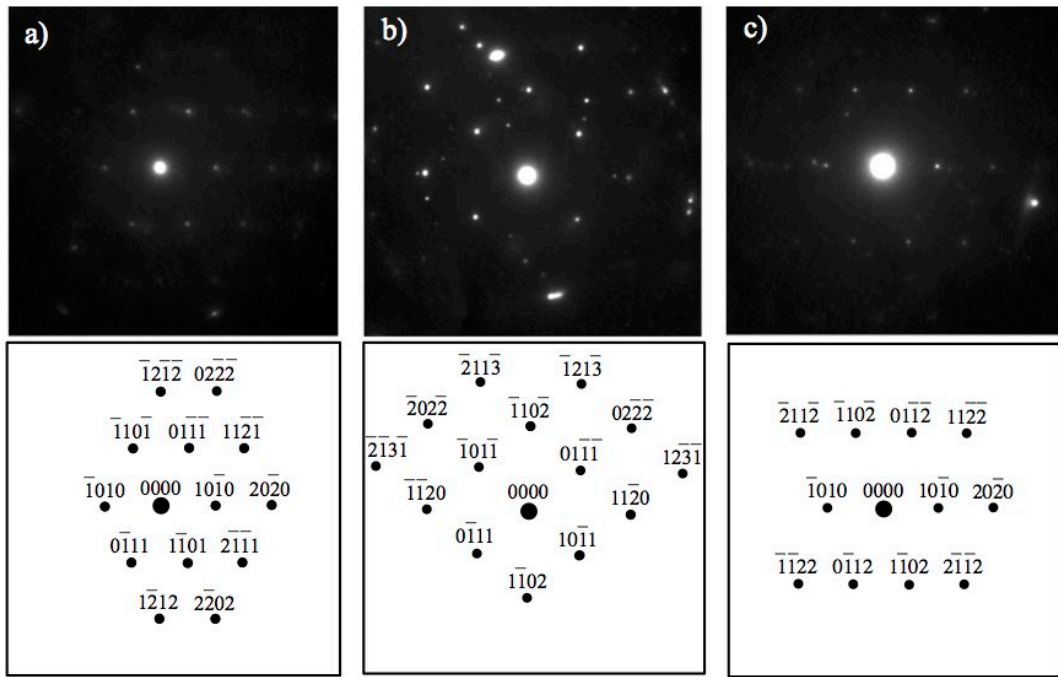


Figure 5. Electron diffraction patterns from $\text{Ti}_2\text{O}_{1-x}$ with the zone axes a) $[\bar{1}2\bar{1}3]$, b) $[\bar{1}\bar{1}101]$ and c) $[\bar{2}4\bar{2}3]$.

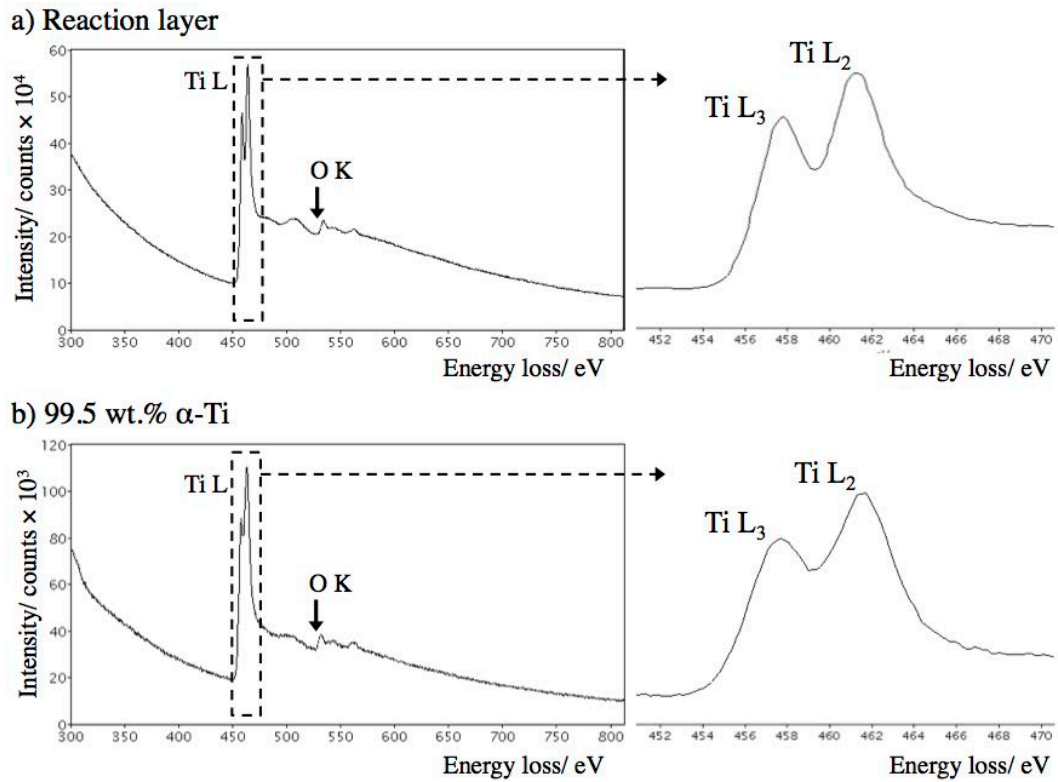


Figure 6. EEL spectra showing the Ti L and O K edges for a) the reaction layer shown in Figure 4 designated Ti_2O_{1-x} and b) 99.5 wt.% α -Ti which contains oxygen as an impurity.

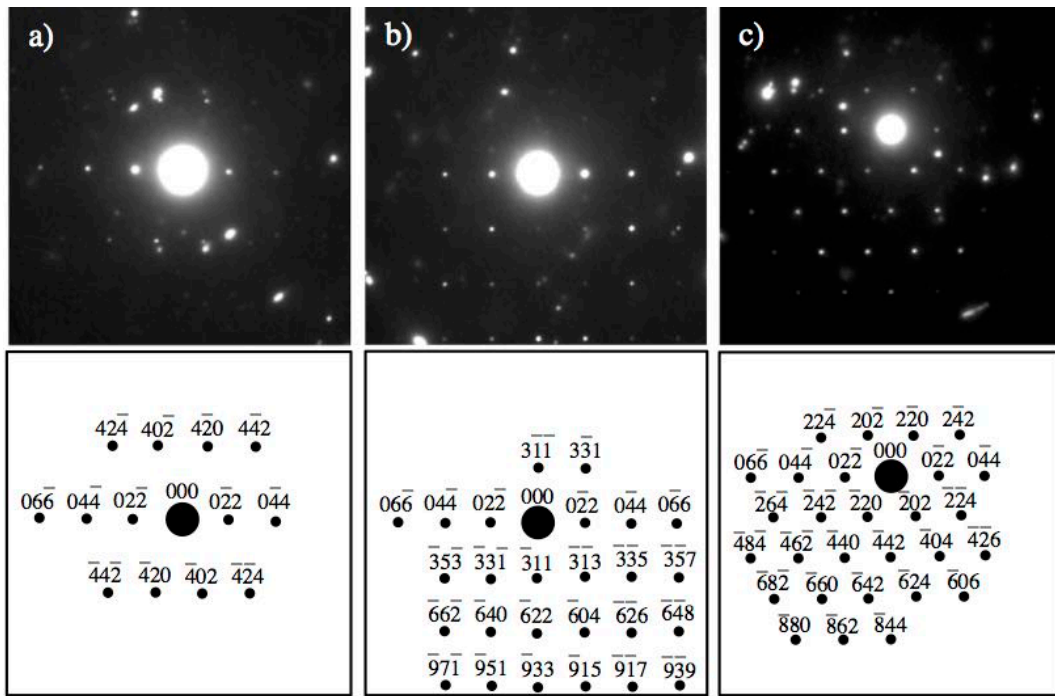


Figure 7. Electron diffraction patterns from $\text{Ti}_3\text{Cu}_3\text{O}$ with the zone axes a) [122], b) [233] and c) [111].

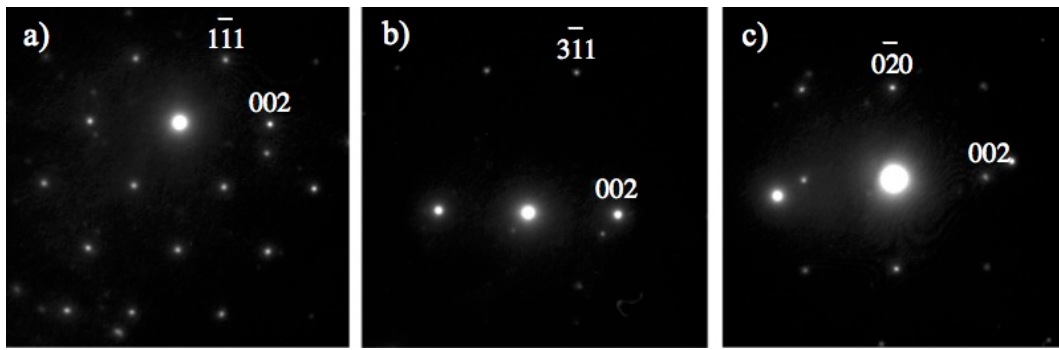


Figure 8. Electron diffraction patterns from γ -TiO with the zone axes a) [110], b) [130] and c) [100].

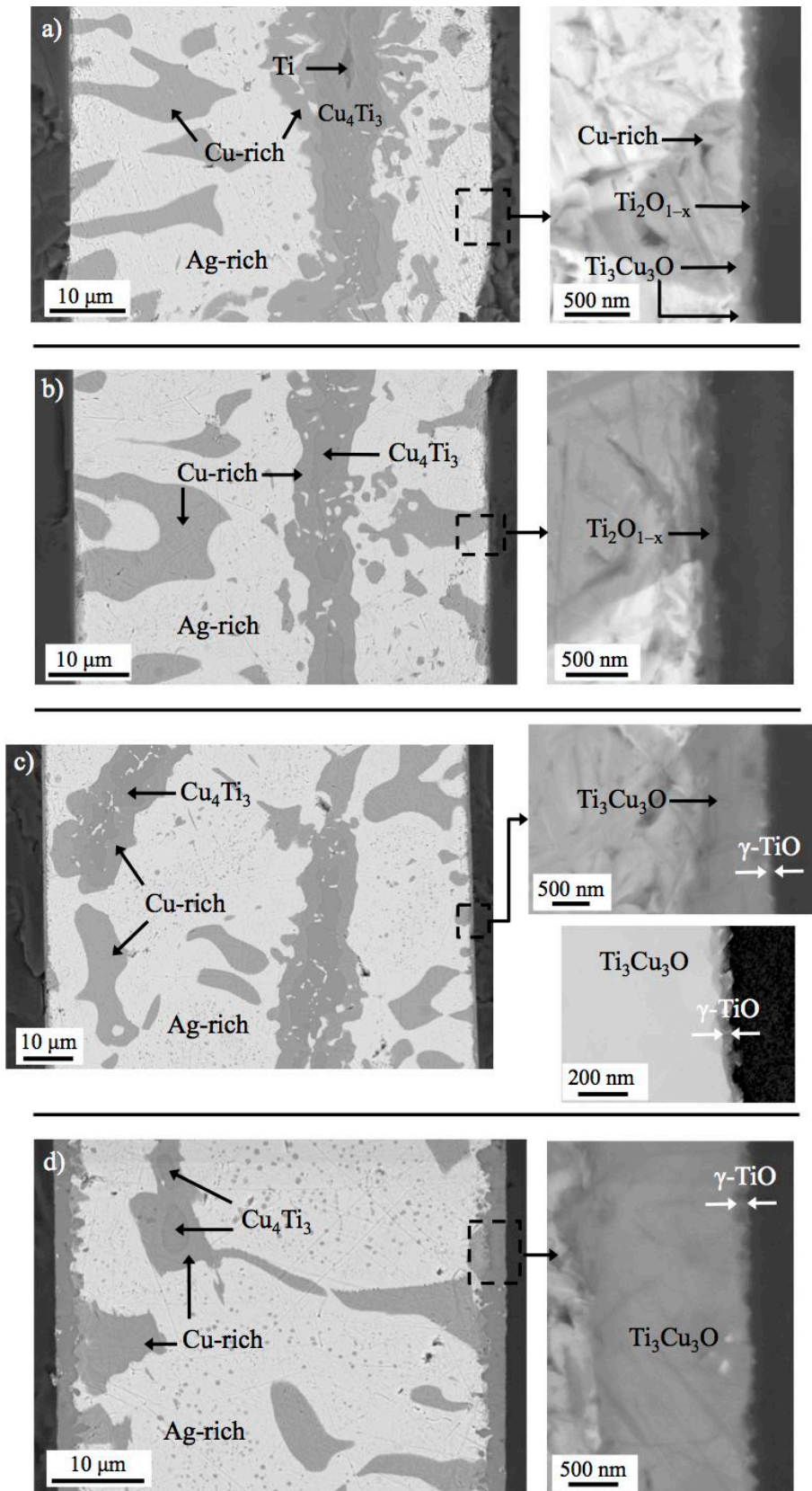


Figure 9. BSEIs of sapphire/Ticasil®/sapphire cross-sections which were held at a) 800 °C, b) 815 °C, c) 845 °C and d) 900 °C for 1 min. A HAADF image is given in c) to clearly show the γ -TiO layer on the sapphire.

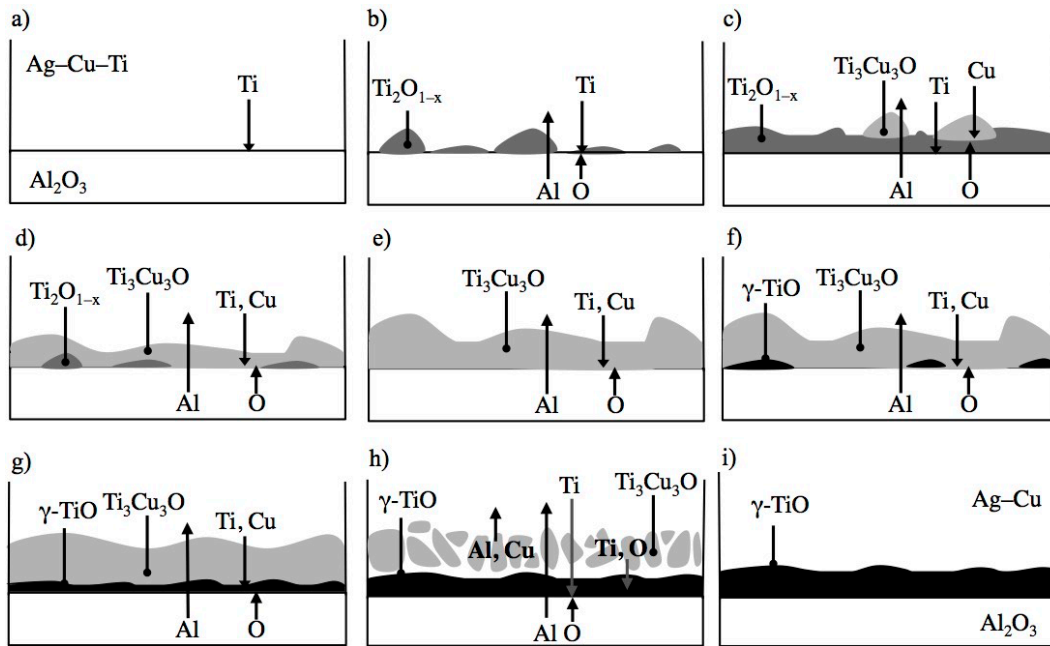


Figure 10. a-f) Schematic mechanism for the evolution of interfacial phases at a Ag-Cu-Ti/sapphire interface during brazing, g-h) along with the effect on the interfacial microstructure of holding at the peak temperature for extended periods of time. a) Melting of the ABA facilitates diffusion of Ti to the surface of the sapphire. b) $\text{Ti}_2\text{O}_{1-x}$ particles nucleate on sapphire to form a broken layer, by equation 3, with Al diffusing into the ABA. c) $\text{Ti}_3\text{Cu}_3\text{O}$ particles nucleate on a continuous $\text{Ti}_2\text{O}_{1-x}$ layer by equation 6. d) Growth of $\text{Ti}_3\text{Cu}_3\text{O}$, primarily parallel to the sapphire surface, forming a continuous layer with further decomposition of $\text{Ti}_2\text{O}_{1-x}$. e) $\text{Ti}_2\text{O}_{1-x}$ has reacted completely by equation 6 to support the growth of the $\text{Ti}_3\text{Cu}_3\text{O}$ layer. f) Nucleation of $\gamma\text{-TiO}$ between $\text{Ti}_3\text{Cu}_3\text{O}$ and the sapphire by equation 7. g) Formation of a continuous $\gamma\text{-TiO}$ layer alongside the $\text{Ti}_3\text{Cu}_3\text{O}$ layer.

Holding at the peak temperature for long periods of time results in h) decomposition of $\text{Ti}_3\text{Cu}_3\text{O}$ and intergranular diffusion of Ti through the $\text{Ti}_3\text{Cu}_3\text{O}$ layer to facilitate rapid growth of $\gamma\text{-TiO}$, and finally i) a single thick continuous $\gamma\text{-TiO}$ layer on the sapphire following complete decomposition of $\text{Ti}_3\text{Cu}_3\text{O}$.